Title

Duration and dynamics of the best orbital analogue to the present interglacial

Journal

Geology, 43(7)

ISSN

0091-7613

Authors

Giaccio, Biagio
Regattieri, Eleonora
Zanchetta, Giovanni
et al.

Publication Date

2015-07-01

DOI

10.1130/g36677.1

Peer reviewed

Duration and dynamics of the best orbital analogue to the present interglacial

Biagio Giaccio[1]*, Eleonora Regattieri[1,2,3], Giovanni Zanchetta[1,2,3], Sebastien Nomade[4], Paul R. Renne[5,6], Courtney J. Sprain[5,6], Russell N. Drysdale[7,8], Polychronis C. Tzedakis[9], Paolo Messina[1], Giancarlo Scardia[1,10], Andrea Sposato[1], and Franck Bassinot[4]

[1]Istituto di Geologia Ambientale e Geoingegneria, Consiglio Nazionale delle Ricerche (CNR), Via Salaria km 29,300, 00015 Monterotondo, Rome, Italy

[2]Dipartimento di Scienze della Terra, Università di Pisa, Via S. Maria 53, 56126 Pisa, Italy

[3]Istituto di Geoscienze e Georisorisorse, Consiglio Nazionale delle Ricerche (CNR),Via Giuseppe Moruzzi 1, 56124 Pisa, Italy

[4]Laboratoire des Sciences du Climat et de l'Environnement (CEA-CNRS-UVSQ), Avenue de la terrasse, Bât 12 91198 Gif Sur Yvette cedex, France

[5]Berkeley Geochronology Center, 2455 Ridge Road, Berkeley, California 94709, USA

[6]Department of Earth and Planetary Science, University of California–Berkeley, Berkeley, California 94720, USA

[7]School of Geography, University of Melbourne, 221 Bouverie Street, Carlton, 3052 Victoria, Australia

[8]Laboratoire EDYTEM (Environnement et Dynamique des Territoires de Montagnes), Université de Savoie, Pôle Montagne, 73376 Le Bourget du Lac cedex, France

[9]Department of Geography, University College London, Pearson Building, Gower Street, London WC1E 6BT, UK

[10]Instituto de Geociências e Ciências Exatas, Universidade Estadual Paulista, Rio Claro, SP 13506-900, Brazil

ABSTRACT

Past orbital analogues to the current interglacial, such as Marine Isotope Stage 19c (MIS 19c, ca. 800 ka), can provide reliable reference intervals for evaluating the timing and the duration of the Holocene and factors inherent in its climatic progression. Here we present the first high-resolution paleoclimatic record for MIS 19 anchored to a high-precision $^{40}Ar/^{39}Ar$ chronology, thus fully independent of any *a priori* assumptions on the orbital mechanisms underlying the climatic changes. It is based on the oxygen isotope compositions of Italian lake sediments showing orbital- to millennial-scale hydrological variability over the Mediterranean between 810 and 750 ka. Our record indicates that the MIS 19c interglacial lasted 10.8 ± 3.7 k.y., comparable to the time elapsed since the onset of the Holocene, and that the orbital configuration at the time of the following glacial inception was very similar to the present one. By analogy, the current interglacial should be close to its end. However, greenhouse gas concentrations at the time of the MIS 19 glacial inception were significantly lower than those of the late Holocene, suggesting that the current interglacial could have already been prolonged by the progressive increase of the greenhouse gases since 8–6 ka, possibly due to early anthropogenic disturbance of vegetation.

INTRODUCTION

The Milankovitch paradigm for the response of Earth's climatic system to astronomical forcing provides the theoretical framework to explain the pacing of interglacial-glacial cycles (Hays et al., 1976). It predicts that the onset of interglacials occurs close to the boreal summer insolation maximum–precession minimum, but glacial inceptions defy the theoretical prediction because they lack a systematic relation to insolation (Tzedakis et al., 2012a). Furthermore, although climate models have demonstrated how the reduction in boreal summer insolation plays a predominant role in glacial inception (Calov et al., 2009), uncertainty regarding the timing of the next glacial onset persists because of the low orbital eccentricity that will characterize the next 100 k.y., resulting in a very subdued amplitude of insolation variability (e.g., Loutre and Berger, 2000).

The study of the past interglacial analogs for the Holocene, or Marine Isotope Stage 1 (MIS 1), may thus be pivotal for evaluating the temporal extent of the present interglacial. Although not perfectly identical to MIS 1, in terms of orbital configuration, insolation distribution pattern, and temperature response, MIS 19 can be considered the closest to the current interglacial (e.g., Yin and Berger, 2012). The MIS 19 interglacial (MIS 19c) is well expressed in marine (Channell et al., 2010) and ice (Jouzel et al., 2007) records. However, the age models of these records are entirely or partially dependent upon astrochronology, and thus the recent estimation of ~12.5 k.y. for the duration of MIS 19c (Tzedakis et al., 2012b) rests on the assumed validity of the orbital tuning approach. In order to address this issue independent of any *a priori* assumptions, we assembled the first high-precision $^{40}Ar/^{39}Ar$ dated high-resolution paleoclimatic record for this interval from Italian lacustrine sediments (Fig. 1), which preserve a history of hydrological variability and temporal progression of the MIS 19c in the Mediterranean area.

*E-mail: biagio.giaccio@cnr.it

METHODS AND RESULTS

Stratigraphy and Lithology of the Investigated Sulmona 6 Unit

Our study focused on the ~30-m-thick basal interval (20–50 m depth) of the Sulmona 6 (SUL6) lacustrine unit (central Apennine, Italy; Fig. 1), spanning the ca. 820–720 ka interval and encompassing the Matuyama-Brunhes geomagnetic reversal (Giaccio et al., 2013; Sagnotti et al., 2014). With the exception of a meter-thick peaty layer in the upper portion of the succession (at ~26 m depth; Fig. 1), the lithology consists of whitish massive to faintly laminate marls that indicate a continuous sedimentation in a relatively deep lake environment. X-ray diffraction and scanning electron microscope analyses reveal that the non-clay fraction of the lacustrine sediments from unit SUL6 is mainly composed of euhedral to subhedral calcite crystals of ~10–15 μm, typical of biogenic precipitation (e.g., Kelts and Hsü, 1978).

Proxy Data and Their Paleoclimatic Interpretation

Both oxygen isotope ratios ($\delta^{18}O$) and percent $CaCO_3$ depth series from the SUL6 unit (Fig. DR1 and methods in the GSA Data Repository[1]) show notable variations that reflect changes in hydrological regime. The

[1]GSA Data Repository item 2015209, additional information on $\delta^{18}O$, $\delta^{13}C$, $CaCO_3$, magnetic susceptibility, and $^{40}Ar/^{39}Ar$ analyses; detailed results of the $^{40}Ar/^{39}Ar$ dating for individual dated tephras; Figures DR1 and DR2; and full analytical details for individual crystals (Data Sets DR1 and DR2), is available online at www.geosociety.org/pubs/ft2015.htm, or on request from editing@geosociety.org or Documents Secretary, GSA, P.O. Box 9140, Boulder, CO 80301, USA.

GEOLOGY, July 2015; v. 43; no. 7; p. 603–606 | Data Repository item 2015209 | doi:10.1130/G36677.1 | Published online 19 May 2015

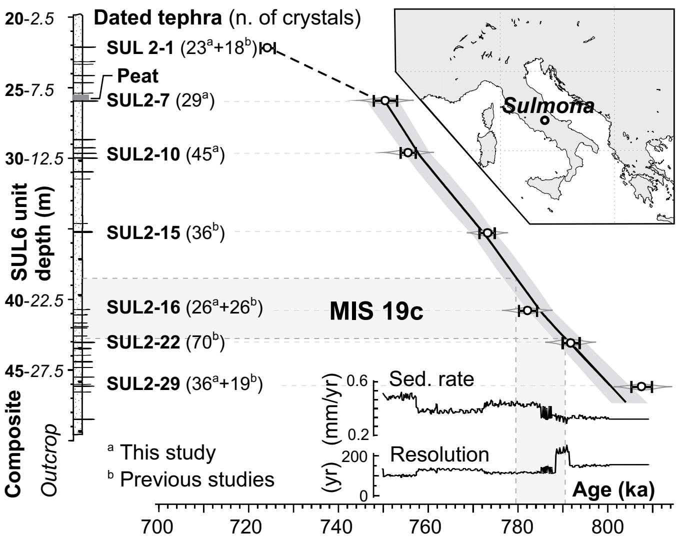

Figure 1. Bayesian age model for the 30-m-thick basal interval of the composite core and outcrop of the Sulmona 6 (SUL6) unit (central Apennines, Italy; Giaccio et al., 2013) (n.—number). For comparison, both composite (bold) and outcrop (italic) depth scales area shown. The depth-age model (thin black line) and corresponding 95% confidence limits (thick gray line) are based on Bacon software (Blaauw and Christen, 2011) applied to $^{40}Ar/^{39}Ar$ dating and corresponding 95% confidence uncertainties (white dots and related error bars; tapered horizontal bars represent the full propagated errors as generated by Bacon software), from both present and previous studies (Table DR1; see footnote 1). The Marine Isotope Stage 19c (MIS 19c) interglacial is recorded in the ~4-m-thick highlighted interval between the depths of ~38.6 m and ~42.7 m. The resulting sedimentation (Sed.) rate and temporal resolution for the oxygen isotope record are also shown. Dashed line represents the interval with uncertain sedimentation rate, not considered for the final age model and proxy records, which includes the lake-level lowstand-related peat layer just above the SUL2–7 tephra. Inset shows the location of the Sulmona basin (42°09′14″N, 13°49′05″E).

$\delta^{18}O$ of carbonates from Mediterranean lakes and caves (speleothems) is an established proxy for regional hydrological variability, which is modulated by the proportion of advected air masses from the North Atlantic to the basin, and thus an indirect expression of the boreal subpolar climate variability (e.g., Roberts et al., 2008).

The content of $CaCO_3$ is related to lake bioproductivity, which is low under glacial and/or stadial climatic conditions, during which the proportion of siliciclastic sedimentary input from rivers is higher, and high during interglacial and/or interstadial periods (Vogel et al., 2010). This is also reflected in the measurements of sediment magnetic susceptibility, which varies as the complement to the carbonate content (Fig. DR1).

Chronology

We refined the previous chronology of the SUL6 unit (Giaccio et al., 2013; Sagnotti et al., 2014) by 6 additional high-precision $^{40}Ar/^{39}Ar$ dates, which yielded 13 ages for 7 different tephras, with small analytical uncertainties of 2‰–3‰ (Fig. 1; Table DR1). Specifically, the ages from five of these tephras were determined by combining the results from paired subsamples dated in two different laboratories, the Berkeley Geochronology Center (Berkeley, California, USA) and CNRS (Centre National de la Recherche Scientifique) Le Laboratoire des Sciences du Climat et de l'Environnement (Gif Sur Yvette, France), each yielding statistically indistinguishable ages (Table DR1; Fig. DR2; analytical details are given in Data Sets DR1 and DR2 in the Data Repository).

The final Bayesian depth-age model was based on the 6 age control points below the peat layer at ~26 m depth (Table DR1), which marks a lake-level lowstand and a possible sedimentation hiatus (Fig. 1). The resulting record spans ~805–750 k.y., with a temporal resolution of 100–200 yr for the $\delta^{18}O$ time series (Fig. 1).

DISCUSSION

The MIS 19 isotope record for Sulmona reproduces in detail the variability observed in the reference records of the European Project for Ice Coring in Antarctica (EPICA) Dome C Antarctic ice (Jouzel et al., 2007) and of planktonic $\delta^{18}O$ from the subpolar North Atlantic Ocean Drilling Program Site 983 (Channell et al., 2010), including a series of abrupt millennial-scale oscillations (Fig. 2). In contrast with these reference records, the Sulmona succession has the advantage of yielding precise ages for estimating the duration of the MIS 19c, independent of any orbital assumptions. Although several calibrations are in use for the $^{40}Ar/^{39}Ar$ method, which yields absolute ages that vary by ~2% in the Pleistocene (e.g., Sagnotti et al., 2014), the chronological resolution of the method, i.e., relative $^{40}Ar/^{39}Ar$ age, is unaffected by uncertainties in absolute calibration and is limited only by analytical precision (~2‰–3‰; Fig. DR2). Furthermore, the Sulmona record also provides indirect but closely related proxy evidence of the North Atlantic millennial-scale variability, which is a key feature for defining interglacial-glacial boundaries (Tzedakis et al., 2012a).

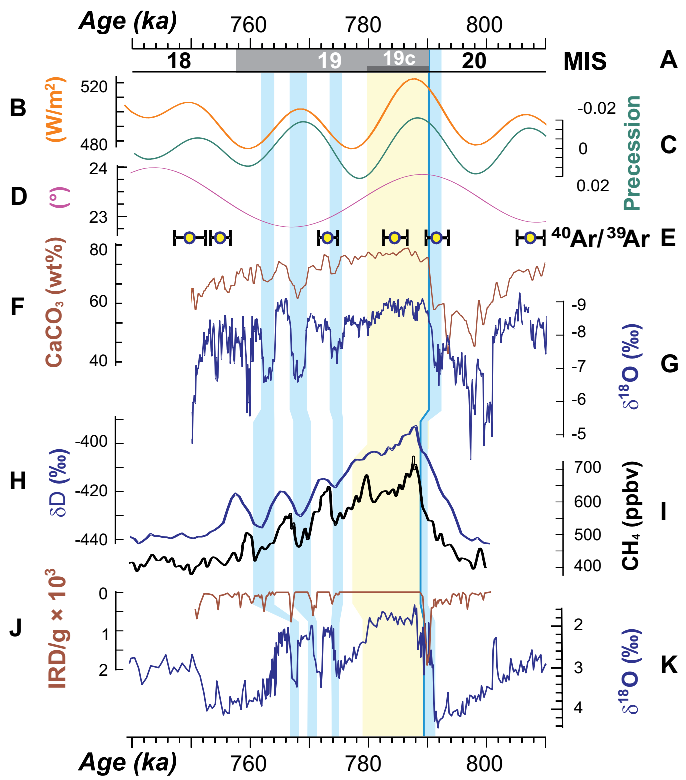

Figure 2. Paleoclimatic records and orbital parameters for the Marine Isotope Stage (MIS) 20–MIS 18 period. A: Marine isotope stages. B: 21 June insolation at 65°N. C: Precession index. A–C are after Berger and Loutre (1991). D: Obliquity. E: $^{40}Ar/^{39}Ar$ ages (2σ analytical error) of the Sulmona (central Apennines, Italy) tephras. F: $CaCO_3$ records from Sulmona basin sediments. G: Oxygen isotope records of Sulmona basin sediments. H: δD in Antarctica European Project for Ice Coring in Antarctica (EPICA) Dome C ice record (Jouzel et al., 2007) on the Antarctic ice core chronology (AICC2012) age model (Bazin et al., 2013). I: Methane concentration in Dome C ice record (Loulergue et al., 2008) on the AICC2012 age model (Bazin et al., 2013). J: Ice-rafted debris (IRD) records from North Atlantic Ocean Drilling Program Site 983 band. K: Planktonic $\delta^{18}O$ records from North Atlantic Ocean Drilling Program Site 983 based on Ocean Drilling Program astrochronological time scale (Kleiven et al., 2011).

While the formal distinction between glacials and interglacials is mostly related to ice volume and sea level, an indirect indication of the growth of the ice sheets is provided by millennial-scale records of ice-rafted debris (IRD) produced by iceberg discharges to the North Atlantic that trigger Northern Hemisphere cold events and bipolar seesaw oscillations (Tzedakis et al., 2012a). These cold events can be traced in Mediterranean marine and terrestrial records as sea-surface cooling (e.g., Martrat et al., 2014) and decreases in precipitation, as revealed by pollen (e.g., Brauer et al., 2007) and lake and speleothem $\delta^{18}O$ (e.g., Regattieri et al., 2015) records. However, both direct and indirect IRD proxy records provide a late indication of glacial inception, because the first IRD events that follow the interglacials occur only once the ice sheets extend to coastlines and reach the critical size for collapsing, millennia after the onset of the ice growth (Tzedakis et al., 2012a). A less ambiguous definition of interglacial onset, analogous to the Holocene (Walker et al., 2012), can be identified from the end of the terminal bipolar seesaw oscillation, or Younger Dryas (YD)–like cold and dry event, of the preceding glacial periods, a pervasive feature of the last nine glacial-interglacial transitions (Broecker et al., 2010; Barker et al., 2011). This notion of interglacial boundaries could differ from the formal one based on ice volume and sea level. Nevertheless, it provides unambiguous stratigraphic criteria for delimiting intervals that approach the length of the sea-level highstands and for consistently comparing different interglacials, the purpose of this paper.

Full interglacial conditions in the Sulmona isotope record occur sharply at the end of the last YD-like drier pulse dated as 790.6 ± 2.5 ka (95% confidence); this pulse interrupts the preceding long-term wetting trend that started ca. 805 ka (Figs. 2G and 3E). Following an ~8-k.y.-long period of relative stability, the Sulmona MIS 19 record shows a progressive ~7-k.y.-long trend of isotope enrichment that culminates in the first marked dry episode that can be correlated with the earliest IRD event in North Atlantic, and thus to the reestablishment of the millennial-scale bipolar seesaw (Fig. 2G). From theoretical considerations, the end of MIS 19c should be within this millennial-long drying trend of the Sulmona record that would represent the local hydrological response to ice sheet growth (Fig. 3E). It is conceivable that it could coincide with the definitive increase of $\delta^{18}O$ beyond ~– 8.4‰ at 779.8 ± 2.8 ka, a value that corresponds to the maximum threshold reached by the minor $\delta^{18}O$ excursions during the period of unambiguous interglacial condition (Fig. 3E). The total duration of the MIS 19c in the Sulmona record derived from our age model is 10.8 ± 3.7 k.y. (2σ; Fig. 3). This duration is robust across other age models, including simple piecewise linear interpolation of age-depth data, which yield a duration of 11.6 ± 2.3 k.y. Although our preferred duration estimate might statistically extend to ~14.5–13.5 k.y. (~4% probability), there is a higher probability that it is within ~12.5–9.0 k.y. (~68%), and thus approaches the astrochronological estimation of the MIS 19c length (~12.5 k.y.; Tzedakis et al., 2012b) as well as the time elapsed since the inception of the Holocene (Fig. 3D).

In order to compare MIS 19 and MIS 1, we synchronized the Sulmona MIS 20–19 and the Late Glacial–Holocene sea surface paleotemperature record from Alboran Sea (Martrat et al., 2014), anchored to the respective orbital parameters, along the abrupt end of the YD-like oscillation, which is clearly documented at the glacial-interglacial transition of both series (Figs. 3D and 3E). In spite of the large uncertainty for the absolute ages of the MIS 19c boundaries, this alignment shows that the overall astronomical configuration for the start and end of MIS 19c is in good agreement with the Milankovitch pacing of the MIS 20–MIS 19 glacial-interglacial transition and replicates well the Holocene configuration (Figs. 3A–3C). Substantial coherence between the two paleoclimatic time periods is also evident, in particular the long-term cooling trend and the minor oscillations in the Alboran Sea record, that have similar hydrological expressions in the MIS 19c in the Sulmona record (Figs. 3D and 3E). Consequently, by analogy between MIS 19c and MIS 1, the current interglacial should be very close to its end. However, when considering

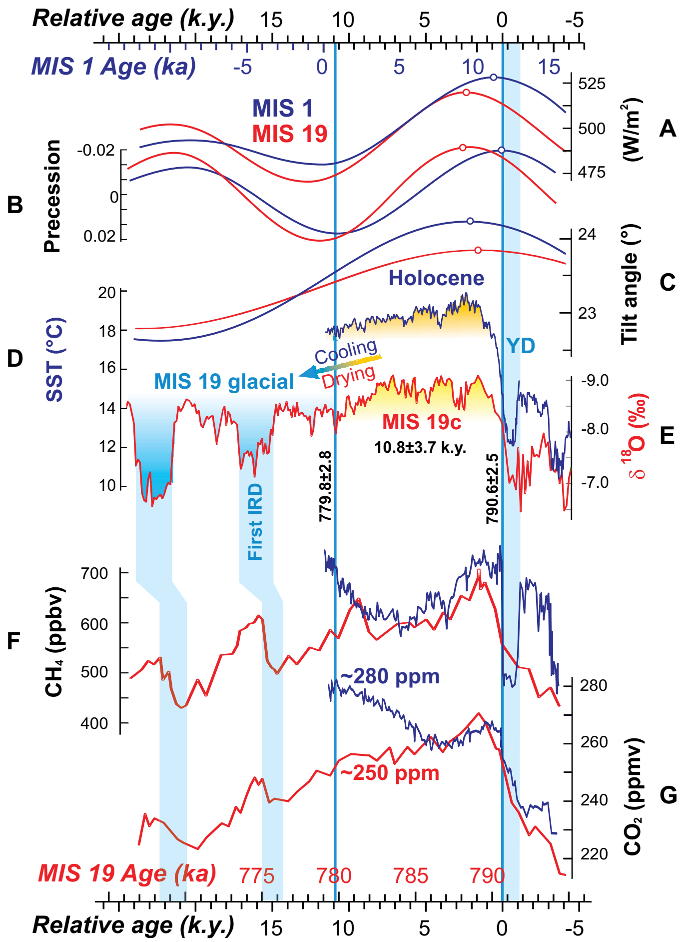

Figure 3. Synchronization of the Marine Isotope stage (MIS) 1 and MIS 19 paleoclimatic records and orbital parameters. Each MIS 1 and MIS 19 time series was constructed on its own age model and aligned along the abrupt end of the Younger Dryas (YD) or YD-like event, as recorded in Alboran Sea and Sulmona (Italy) records, respectively, assumed as time zero of the relative time scale. IRD—ice-rafted debris. A: 21 June insolation at 65°N. B: Precession index. C: Obliquity. A–C are after Berger and Loutre (1991). D: Late Glacial–Holocene sea-surface temperature (SST) record from Alboran Sea (Martrat et al., 2014). E: Late MIS 20–MIS 19 oxygen isotope records from Sulmona lake sediments. F: Methane concentrations in Late Glacial–Holocene record from Greenland North Greenland Ice Core Project (NGRIP) core (EPICA Community Members, 2006), and in late MIS 20–MIS 19 from Antarctica European Project for Ice Coring in Antarctica (EPICA) Dome C ice record (Loulergue et al., 2008), on the Antarctic ice core chronology (AICC2012) age model (Bazin et al., 2013). G: Carbon dioxide concentration in Late Glacial–Holocene (Monnin et al., 2004) and late MIS 20–MIS 19 (Bereiter et al., 2015) from the Antarctic Dome C core.

the other relevant factors required for triggering a glacial inception, i.e., the atmospheric greenhouse gas concentrations (e.g., CO_2), a substantial difference between MIS 19 and MIS 1 emerges. At the time of the MIS 19 glacial inception, the corresponding CO_2 content in EPICA Dome C ice was ~250 ppm (Bereiter et al., 2015; Fig. 3G), while the preindustrial concentration of CO_2 was ~280 ppm; over the entire Holocene it never fell below ~260 ppm, which was reached ca. 8–6 ka (Monnin et al., 2004; Fig. 3G). However, according to the early anthropogenic hypothesis (Ruddiman, 2007), in the absence of early agricultural greenhouse gas emissions, the late Holocene CO_2 levels should have fallen to ~245 ppm, i.e., close to the value observed near the end of MIS 19c. The case of delayed or failed glaciation caused by the progressive, possibly anthropogenic, increase of atmospheric CO_2 concentrations since ca. 8–6 ka would seem to be supported by the results of our study.

CONCLUDING REMARKS

The Sulmona record provides the first independent radioisotopic validation of the astrochronological time scales of ice core and marine records for the MIS 19c and thus of the previous estimation of its length deduced from these time series.

The MIS 19c and MIS 1 comparison suggests that the variability and the total duration of MIS 19c interglacial in our record (10.8 ± 3.7 k.y., 2σ) are comparable to those of the elapsed period since onset of the current interglacial (ca. 11.7 ka) and that the astronomical configuration required for driving the MIS 1 glacial inception should have already been reached. However, the expected shifting of the late Holocene climate system into a glacial period might have been delayed or inhibited by the relatively higher levels of the CO_2 concentration. Regardless of the remaining uncertainty on the causes underlying the difference in greenhouse gas levels during the MIS 19 and the preindustrial-Holocene (i.e., early anthropogenic hypothesis versus natural), this would have been enough to drastically deviate the evolutionary climatic trajectories of the two orbital analog interglacials, highlighting a very high sensitivity of the climate to greenhouse gases.

ACKNOWLEDGMENTS

We thank Valerie Masson-Delmotte for her critical review of an early manuscript. We also benefited from insightful comments from Bill Ruddiman and five anonymous reviewers. Regattieri is supported by a Ph.D. grant from the School of Graduate Studies Galileo Galilei (University of Pisa, Italy). The $^{40}Ar/^{39}Ar$ ages were supported by the Ann and Gordon Getty Foundation (Berkeley Geochronology Center), and by a SYSTER 2013 program from the National Institute for Earth Sciences and Astronomy (CNRS-INSU) to Nomade. Tzedakis acknowledges funding from the Natural Environment Research Council (grant NE/I025115/1). Giaccio thanks La Locanda di Gino in Sulmona, Italy, for valuable help in the field.

REFERENCES CITED

Barker, S., Knorr, G., Lawrence Edwards, R., Parrenin, F., Putnam, A.E., Skinner, L.C., Wolff, E., and Ziegler, M., 2011, 800,000 years of abrupt climate variability: Science, v. 334, p. 347–351, doi:10.1126/science.1203580.

Bazin, L., et al., 2013, An optimized multi-proxy, multi-site Antarctic ice and gas orbital chronology (AICC2012): 120–800 ka: Climate of the Past, v. 9, p. 1715–1731, doi:10.5194/cp-9-1715-2013.

Bereiter, B., Eggleston, S., Schmitt, J., Nehrbass-Ahles, C., Stocker, T.F., Fischer, H., Kipfstuhl, S., and Chappellaz, J., 2015, Revision of the EPICA Dome C CO_2 record from 800 to 600 kyr before present: Geophysical Research Letters, v. 42, p. 542–549, doi:10.1002/2014GL061957.

Berger, A., and Loutre, M.F., 1991, Insolation values for the climate of the last 10 million years: Quaternary Science Reviews, v. 10, p. 297–317, doi:10.1016/0277-3791(91)90033-Q.

Blaauw, M., and Christen, J.A., 2011, Flexible paleoclimate age-depth models using an autoregressive gamma process: Bayesian Analysis, v. 6, p. 457–474, doi:10.1214/ba/1339616472.

Brauer, A., Allen, J.R.M., Mingram, J., Dulski, P., Wulf, S., and Huntley, B., 2007, Evidence for the last interglacial chronology and environmental change from southern Europe: National Academy of Sciences Proceedings, v. 104, p. 450–455, doi:10.1073/pnas.0603321104.

Broecker, W.S., Denton, G.H., Edwards, R.L., Cheng, H., Richard, B., Alley, R.B., and Putnam, A.E., 2010, Putting the Younger Dryas cold event into context: Quaternary Science Reviews, v. 29, p. 1078–1081, doi:10.1016/j.quascirev.2010.02.019.

Calov, R., Ganopolski, A., Kubatzki, C., and Claussen, M., 2009, Mechanisms and time scales of glacial inception simulated with an Earth system model of intermediate complexity: Climate of the Past, v. 5, p. 245–258, doi:10.5194/cp-5-245-2009.

Channell, J.E.T., Hodell, D.A., Singer, B.S., and Xuan, C., 2010, Reconciling astrochronological and $^{40}Ar/^{39}Ar$ ages for the Matuyama-Brunhes boundary and late Matuyama Chron: Geochemistry, Geophysics, Geosystems, v. 11, Q0AA12, doi:10.1029/2010GC003203.

EPICA Community Members, 2006, One-to-one coupling of glacial climate variability in Greenland and Antarctica: Nature, v. 444, p. 195–198, doi:10.1038/nature05301.

Giaccio, B., Castorina, F., Nomade, S., Scardia, G., Voltaggio, M., and Sagnotti, L., 2013, Revised chronology of the Sulmona lacustrine succession, central Italy: Journal of Quaternary Science, v. 28, p. 545–551, doi:10.1002/jqs.2647.

Hays, J.D., Imbrie, J., and Shackleton, N.J., 1976, Variations in the Earth's orbit: Pacemaker of the ice ages: Science, v. 194, p. 1121–1132, doi:10.1126/science.194.4270.1121.

Jouzel, J., et al., 2007, Orbital and millennial Antarctic climate variability over the past 800,000 years: Science, v. 317, p. 793–796, doi:10.1126/science.1141038.

Kelts, K., and Hsü, K.J., 1978, Freshwater carbonate sedimentation, *in* Lerman, A., ed., Lakes—Chemistry, geology, physics: Berlin, Springer-Verlag, p. 295–323.

Kleiven, H.F., Hall, I.R., McCave, I.N., Knorr, G., and Jansen, E., 2011, Coupled deep-water flow and climate variability in the middle Pleistocene North Atlantic: Geology, v. 39, p. 343–346, doi:10.1130/G31651.1.

Loulergue, L., Schilt, A., Spahni, R., Masson-Delmotte, V., Blunier, T., Lemieux, B., Barnola, J.-M., Raynaud, D., Stocker, T.F., and Chappellaz, J., 2008, Orbital and millennial-scale features of atmospheric CH_4 over the past 800,000 years: Nature, v. 453, p. 383–386, doi:10.1038/nature06950.

Loutre, M.F., and Berger, A., 2000, Future climatic changes: Are we entering an exceptionally long interglacial?: Climatic Change, v. 46, p. 61–90, doi:10.1023/A:1005559827189.

Martrat, B., Jimenez-Amat, P., Zahn, R., and Grimalt, J.O., 2014, Similarities and dissimilarities between the last two deglaciations and interglaciations in the North Atlantic region: Quaternary Science Reviews, v. 99, p. 122–134, doi:10.1016/j.quascirev.2014.06.016.

Monnin, E., et al., 2004, Evidence for substantial accumulation rate variability in Antarctica during the Holocene, through synchronization of CO_2 in the Taylor Dome, Dome C and DML ice cores: Earth and Planetary Science Letters, v. 224, p. 45–54, doi:10.1016/j.epsl.2004.05.007.

Regattieri, E., Giaccio, B., Zanchetta, G., Drysdale, R.S., Galli, P., Peronace, E., Nomade, S., and Wulf, S., 2015, Hydrological variability over Apennine during the Early Last Glacial precession minimum, as revealed by a stable isotope record from Sulmona basin, central Italy: Journal of Quaternary Science, v. 30, p. 19–31, doi:10.1002/jqs.2755.

Roberts, N., et al., 2008, Stable isotope records of late Quaternary climate and hydrology from Mediterranean lakes: The ISOMED synthesis: Quaternary Science Reviews, v. 27, p. 2426–2441, doi:10.1016/j.quascirev.2008.09.005.

Ruddiman, W.F., 2007, The early anthropogenic hypothesis: Challenges and responses: Reviews of Geophysics, v. 45, RG4001, doi:10.1029/2006RG000207.

Sagnotti, L., Scardia, G., Giaccio, B., Liddicoat, J.C., Nomade, S., Renne, P.R., and Sprain, C.J., 2014, Extremely rapid directional change during Matuyama-Brunhes geomagnetic polarity reversal: Geophysical Journal International, v. 199, p. 1110–1124, doi:10.1093/gji/ggu287.

Tzedakis, P.C., Wolff, E.W., Skinner, L.C., Brovkin, V., Hodell, D.A., McManus, J.F., and Raynaud, D., 2012a, Can we predict the duration of an interglacial?: Climate of the Past, v. 8, p. 1473–1485, doi:10.5194/cp-8-1473-2012.

Tzedakis, P.C., Channell, J.E.T., Hodell, D.A., Kleiven, H.F., and Skinner, L.C., 2012b, Determining the natural length of the current interglacial: Nature Geoscience, v. 5, p. 138–141, doi:10.1038/ngeo1358.

Vogel, H., Zanchetta, G., Sulpizio, R., Wagner, B., and Nowaczyk, N.A., 2010, Tephrostratigraphic record for the last glacial-interglacial cycle from Lake Ohrid, Albania and Macedonia: Journal of Quaternary Science, v. 25, p. 320–338, doi:10.1002/jqs.1311.

Walker, M.J.C., Berkelhammer, M., Björck, S., Cwynar, L.C., Fisher, D.A., Long, A.J., Lowe, J.J., Newnham, R.M., Rasmussen, S.O., and Weiss, H., 2012, Formal subdivision of the Holocene Series/Epoch: A discussion paper by a working group of INTIMATE (Integration of Ice-Core, Marine and Terrestrial Records) and the Subcommission on Quaternary Stratigraphy (International Commission on Stratigraphy): Journal of Quaternary Science, v. 27, p. 649–659, doi:10.1002/jqs.2565.

Yin, Q.Z., and Berger, A., 2012, Individual contribution of insolation and CO_2 to the interglacial climates of the past 800,000 years: Climate Dynamics, v. 38, p. 709–724, doi:10.1007/s00382-011-1013-5.

Manuscript received 5 February 2015
Revised manuscript received 21 April 2015
Manuscript accepted 24 April 2015

Printed in USA

Geology

Duration and dynamics of the best orbital analogue to the present interglacial

Biagio Giaccio, Eleonora Regattieri, Giovanni Zanchetta, Sebastien Nomade, Paul R. Renne, Courtney J. Sprain, Russell N. Drysdale, Polychronis C. Tzedakis, Paolo Messina, Giancarlo Scardia, Andrea Sposato and Franck Bassinot

Geology 2015;43;603-606
doi: 10.1130/G36677.1

Notes